A Model for Anesthetic Washout During Recovery in the Post Anesthesia Care Unit

Cameron Jacobson
Department of Bioengineering, University of Utah, Salt Lake City, UT

***Abstract*—Hypercapnia with hyperventilation during emergence from anesthesia has been shown to reduce emergence time, yet little is known about how the subsequent recovery in the post anesthesia care unit (PACU) is affected. A mathematical model has been developed to investigate how inhaled anesthetic agents wash out of patients during recovery in order to demonstrate any difference that hypercapnia and hyperventilation during emergence might have on recovery.**

I. Introduction

GENERAL anesthesia is composed of four phases: induction, maintenance, emergence, and recovery. During the induction phase, patients are placed in an anesthetized state and intubated in preparation for surgery. Maintenance is the continual administration and monitoring of anesthesia during surgery. At the end of surgery, anesthesia is discontinued and the patient is ventilated until they emerge from anesthesia, i.e. their anesthetic level is such that they regain consciousness and breathe spontaneously. Lastly, they are extubated and transported to the PACU for recovery.

The durations of the emergence and recovery phases are influenced by several factors: demographics, surgery length, anesthetic type, hemodynamics, and ventilation. First, demographics, especially body type, can affect how anesthetic is stored in the tissues of the body, e.g. fatty tissues store large amounts of anesthetic compared to other tissue types, hence, washout of the anesthetic can differ from patient to patient. Second, surgery length directly affects how long tissues are exposed to anesthetic agent. Third, anesthetic solubility is a measure of how easily anesthetic dissolves in blood and differs from agent to agent. For example, desflurane has a blood/gas solubility coefficient of 0.45, sevoflurane 0.65, and isoflurane 1.40[1], [2]. As a result desflurane washes out faster than sevoflurane, and sevoflurane washes out faster than isoflurane. Lastly, hemodynamics and ventilation affect the way in which gases, including anesthetics, enter, exit, and move throughout the body.

The cardiovascular and respiratory systems work in tandem to provide the necessary gas exchange for cellular metabolic activity throughout the body. The respiratory system exchanges O_2 and CO_2 between the atmosphere and blood; the circulatory system delivers the O_2 to the cells throughout the body and transports CO_2, a byproduct of cellular respiration, from the cells back to the lungs. When the concentration of CO_2 in the blood fluctuates, the cardiovascular and respiratory systems are adjusted to compensate. For example, if the arterial partial pressure of CO_2 ($PaCO_2$) rises—due to exercise or some kind of strenuous activity—breathing rate and cardiac output will increase and vasodilation will occur, causing an increasing in blood flow and gas exchange in the lungs in order to flush the body of excess CO_2. When $PaCO_2$ decreases, the opposite occurs. In the operating room, this principle is frequently taken advantage of in an effort to accelerate recovery from anesthesia.

Induced hypercapnia, or elevated $PaCO_2$, can be used to accelerate a patient's recovery by washing anesthetic vapors from the body in the same way that excess CO_2 is removed[3], [4]. Hypercapnia during emergence has two important consequences: it increases cerebral blood flow—helping to quickly wash anesthetic from the brain; and it stimulates respiratory drive[5], [6], [7]. Coupled with hyperventilation, a patient is able to expel anesthetic vapors quickly and emerge from anesthesia sooner with a stronger respiratory drive.

A device, developed in our lab, called the QED-100 (Anecare, Salt Lake City, UT), is used to accomplish this task in many hospitals today[8]. The QED-100 incorporates a rebreathing reservoir to induce hypercapnia and a charcoal filter to capture expelled anesthetic gases. The QED-100 is capable of reducing emergence time by approximately 55%[8], [9], [10]. This result translates not only into a cost savings from less time spent in the OR, but perhaps more importantly, it produces a patient that can enter the PACU with less anesthetic in their system and a stronger respiratory drive, which in turn could lead to a faster, safer, and more satisfactory recovery.

The incidence rate of complications in the OR and PACU were estimated to be 1.3-5.1% and 23-24% respectively based on a collection of over 42,000 patients[11], [12], [13]. PONV and upper airway support were the most common events encountered in the PACU, *each* accounting for roughly 1/3 of all PACU complications (2/3 combined). One of the possible reasons for the increased rate of complications in the PACU may stem from the fact that as patients become more alert, they become more aware of pain and often require additional analgesic for pain management. Analgesics can react synergistically with residual inhaled anesthetic still present in the patient's body, similar to how they react during the induction phase of anesthesia, which can result in adverse clinical events (e.g. respiratory depression or even loss of consciousness). Of course, there are several other factors contributing to the likelyhood of complications in the PACU: surgery type, surgery length, ASA physical status, and anesthetic technique[11], [13]. However, aside from these factors, it stands to reason that a patient entering the PACU with less anesthetic in their

system may have a greater chance of avoiding complications.

While it has been shown that hypercapnia with hyperventilation shortens emergence time by removing inhaled anesthetic quickly, the actual levels of anesthetic that patients endure during recovery are not well known. A study, already in progress, has been designed to collect this data, which will then be used to validate the model for anesthetic washout.

Lerou *et al.* described a mathematical model for the uptake and distribution of inhaled anesthetic in a closed-circuit system[1]. A similar model has been developed to simulate not only uptake and distribution of anesthetic agent, but also washout after the breathing circuit has been removed and the patient is breathing spontaneously. Such a model will provide estimates of agent concentration throughout the body that would be difficult to attain through direct measurement—the most important one being cerebral concentration.

In Gopalikrishnan's disseration, he used a similar model to determine cerebral concentrations of anesthetic agent during emergence in order to estimate wake up times[14]. He was able to show that hypercapnia with hyperventilation during emergence quickly reduced the cerebral concentration of anesthetic agent, resulting in a faster wake up time. Likewise, an analogous method will be implemented in order to determine the cerebral concentration of anesthetic agent during key points of recovery. Such a model will provide information that could aid in the developement of a hypercapnia-inducing device for the PACU or simply decision support for clinical staff.

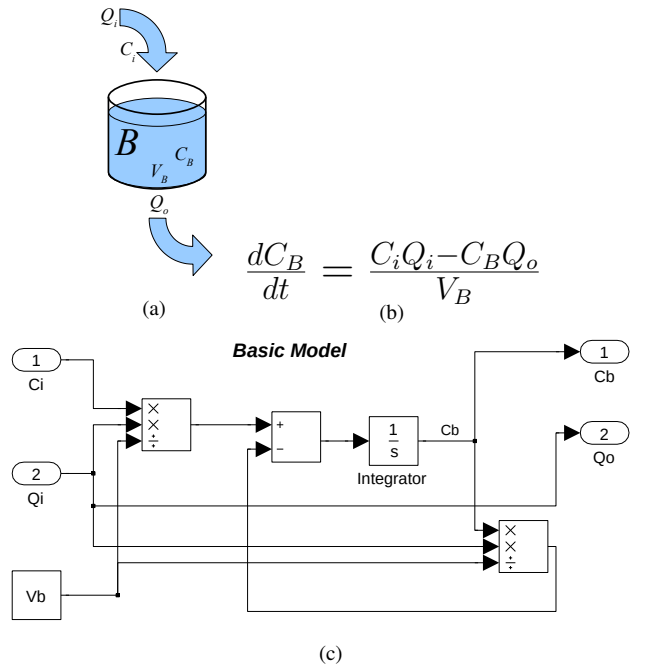

Fig. 1. The basic model. (a) Diagram of the basic model showing a compartment B, with known volume V_B, and concentration of solute C_B, also having incoming flow Q_i with concentration C_i and out going flow Q_o with concentration C_B. (b) Ordinary differential equation describing the rate of change in concentration C_B. (c) Simulink model that describes the equation in (b).

II. Methods

The mathematical model is based on a similar model described and clinically validated by Lerou, *et al.* [1], [15]. It consists of 13 compartments that each represent a particular tissue type or blood pool in the body. Each compartment is fashioned from a basic model where a solute of known concentration flows into a compartment of known volume, having also an outlet with known flow (Figure 1(a)). The ordinary differential equation describing such a scenario is given Figure 1(b) where V_B is the volume of the compartment, C_i is the concentration of the incoming solute with flow rate Q_i, and C_B is the concentration in the compartment and outgoing solute with flow Q_o.

From this basic model, a network of compartments was constructed to simulate the flow of solute through the various tissue groups and blood pools of the body. The solute in this model is the inhaled anesthetic desflurane. As described in Figure 2, the agent is taken in through the lungs, then into the arterial blood pool—blood pools in the model introduce a time delay to simulate circulation time. The arterial blood distributes the anesthetic agent to the various tissue groups, which then empty into the venous blood pool before returning to the lungs.

A data set collected from patients during surgery and recovery from anesthesia will be used to validate the model. This step is currently underway. Following IRB approval, 44 patients undergoing eye muscle surgery will be randomly divided in to two groups: a treatment group, which will be hypercapnic and hypervenilated during emergence; and a control group. End tidal CO_2 ($EtCO_2$), end tidal and inspired anesthetic agent concentration, and minute volume (MV) will be recorded during surgery and recovery. This data will be used to drive the model to simulate induction, maintenance, and emergence phases of anesthesia. In this way, the model will be preloaded with the correct amounts of agent so that washout during recovery can be simulated accurately.

From the patient demographics, lean body weight (LBW) will be estimated as

$$LBW = (1.1 \times BW - \frac{128 \times BW^2}{(100 \times H)^2} \text{ (male)}$$

$$LBW = (1.07 \times BW - \frac{148 \times BW^2}{(100 \times H)^2} \text{ (female)}$$

where BW is measured body weight and H is measured height[16]. Subsequantly, several other physiological values will be derived from LBW for the model: blood volume, tissue volumes, cardiac output, alveolar space, etc[1]. A summary of the variables, symbols, and their relationships are given in Table I.

Using the basic model as a template (Figure 1(b)), the equation describing the rate of change in agent concentration for the alveolar space is

$$\frac{dC_A}{dt} = \frac{(Des - C_A)MV + (C_V - C_{a'})Q_L}{V_A}.$$

The first term in the numerator describes the net change in concentration due to inhalation and exhalation of the gaseos agent; the second term describes the change in terms of the

TABLE I
SYMBOLS AND RELATIONSHIPS AMONG VARIABLES[1], [2]

Variable	Description	Relationship \Value
	Demographics	
A	age (y)	—
BW	body weight (kg)	—
H	height (m)	—
	Fractional Concentrations	
C_a	agent leaving arterial pool	$\frac{dC_a}{dt} = \frac{Q_{CO}(C_{a''} - C_a)}{V_{bla}}$
$C_{a'}$	agent in blood exposed to alveolar gas	$C_{a'} = \lambda_b C_A$
$C_{a''}$	agent entering arterial pool	$C_{a''} = C_{a'}(1 - Q_{fs}) + C_v Q_{fs}$
C_A	agent in alveolar gas	$\frac{dC_A}{dt} = \frac{(Des - C_A)MV + (C_V - C_{a'})Q_L}{V_A}$
C_{at}	agent leaving adipose tissue	$\frac{dC_{at}}{dt} = \frac{(C_a - C_{at})Q_{at}}{V_{at}\lambda_{at}}$
C_b	agent leaving brain tissue	$\frac{dC_b}{dt} = \frac{(C_a - C_b)Q_b}{V_b\lambda_b}$
C_{ct}	agent leaving connective tissue	$\frac{dC_{ct}}{dt} = \frac{(C_a - C_{ct})Q_{ct}}{V_{ct}\lambda_{ct}}$
C_h	agent leaving heart tissue	$\frac{dC_h}{dt} = \frac{(C_a - C_h)Q_h}{V_h\lambda_h}$
C_k	agent leaving kidney tissue	$\frac{dC_k}{dt} = \frac{(C_a - C_k)Q_k}{V_k\lambda_k}$
C_l	agent leaving liver tissue	$\frac{dC_l}{dt} = \frac{(C_a - C_l)Q_l}{V_l\lambda_l}$
C_m	agent leaving muscle tissue	$\frac{dC_m}{dt} = \frac{(C_a - C_m)Q_m}{V_m\lambda_m}$
$C_{vpa'}$	agent leaving venous pool: adipose tissue	$\frac{dC_{vpa'}}{dt} = \frac{(C_{at} - C_{vpa'})Q_{at}}{V_{vpa}}$
C_{vpl}	agent entering venous pool: lean tissue	$C_{vpl} = \frac{C_m Q_m + C_{ct} Q_{ct}}{Q_m + Q_{ct}}$
$C_{vpl'}$	agent leaving venous pool: lean tissue	$\frac{dC_{vpl'}}{dt} = \frac{(C_{vpl} - C_{vpl'})(Q_m + Qct)}{V_{vpl}}$
C_{vpv}	agent entering venous pool: viscera	$C_{vpv} = \frac{C_b Q_b + C_h Qh + C_k Q_k + C_l Q_l}{Q_b + Q_h + Q_k + Q_l}$
$C_{vpv'}$	agent leaving venous pool: viscera	$\frac{dC_{vpv}}{dt} = \frac{(C_{vpv} - C_{vpv'})(Q_b + Q_h + Q_k + Q_l)}{V_{vpv}}$
C_v	agent leaving central venous pool	$\frac{dC_v}{dt} = \frac{(C_{v'} - C_v)Q_{CO}}{V_{vpc}}$
$C_{v'}$	agent entering central venous pool	$C_{v'} = \frac{C_{vpv'}(Q_b + Q_h + Q_k + Q_l) + C_{vpl'}(Q_m + Q_{ct}) + C_{vpa'}Q_{at}}{Q_{CO}}$
Des	agent in inspired air	recorded concentration in Aim 1
	Flows (L/min)	
MV	minute volume	recorded MV in Aim 1
Q_{at}	flow through adipose tissue	$Q_{at} = 0.05 \times Q_{CO}$
Q_b	flow through brain tissue	$Q_b = 0.16 \times Q_{CO}$
Q_{CO}	cardiac output	$Q_{CO} = 0.2 \times LBW$
Q_{ct}	flow through connective tissue	$Q_{ct} = 0.06 \times Q_{CO}$
Q_{fs}	flow through pulmonary shunt	0.05
Q_h	flow through heart tissue	$Q_h = 0.05 \times Q_{CO}$
Q_k	flow through kidney tissue	$Q_k = 0.25 \times Q_{CO}$
Q_l	flow through liver tissue	$Q_l = 0.3 \times Q_{CO}$
Q_m	flow through muscle tissue	$Q_m = 0.13 \times Q_{CO}$
	Volumes (L)	
FRC	function residual volume	$FRC = 0.65(2.34H + 0.009A - 1.090)$ [male]
FRC	function residual volume	$FRC = 0.65(2.24H + 0.001A - 1)$ [female]
V_A	alveolar space	$V_A = FRC + 0.8V_t + V_L\lambda_b\lambda_L$
V_{at}	adipose tissue blood	$V_{at} = 0.15 \times LBW$
V_b	brain tissue blood	$V_b = 0.021 \times LBW$
V_{bl}	total blood	$V_{bl} = 0.07 \times LBW$
V_{bla}	arterial blood	$V_{bla} = 0.2 \times V_{bl}$
V_{blv}	venous blood	$V_{blv} = 0.8 \times V_{bl}$
V_{ct}	connective tissue blood	$V_{ct} = 0.26 \times LBW$
V_d	dead space	$V_d = 0.002 \times LBW$
V_h	heart tissue blood	$V_h = 0.004 \times LBW$
V_k	kidney tissue blood	$V_k = 0.004 \times LBW$
V_L	lung tissue blood	$V_L = 0.008 \times LBW$
V_l	liver tissue blood	$V_l = 0.057 \times LBW$
V_m	muscle tissue blood	$V_m = 0.426 \times LBW$
V_{vpa}	venous pool: adipose tissue	$V_{vpa} = 0.111 \times V_{blv}$
V_{vpc}	central venous pool	$V_{vpc} = 0.126 \times V_{blv}$
V_{vpl}	venous pool: lean tissue	$V_{vpl} = 0.364 \times V_{blv}$
V_{vpv}	venous pool: viscera	$V_{vpv} = 0.399 \times V_{blv}$
V_t	tidal volume	mean of recorded TV in Aim 1
	Partition Coefficients for Desflurane	
λ_{at}	tissue-blood in adipose tissue	29.0
λ_B	blood-gas	0.45
λ_b	tissue-blood in brain tissue	1.22
λ_{ct}	tissue-blood in connective tissue	1.40
λ_h	tissue-blood in heart tissue	1.22
λ_k	tissue-blood in kidney tissue	0.89
λ_L	tissue-blood in lung tissue	1.30
λ_l	tissue-blood in liver tissue	1.49
λ_m	tissue-blood in muscle tissue	1.73

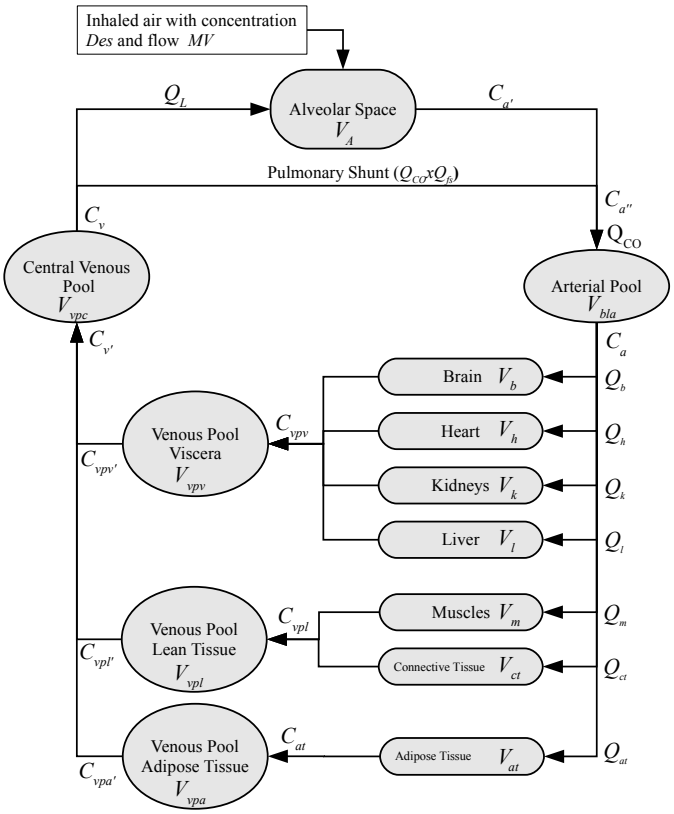

Fig. 2. The 13 compartment model to simulate the uptake, distribution, and washout of inhaled anesthetic agent. See Table I for variable descriptions and relationships.

liquid agent in the blood stream using the appropriate blood-gas partition coefficient for desflurane and noting that $C_{a'} = \lambda_B C_A$. As blood leaves the lungs, it mixes with the blood from the pulmonary shunt. This mixture enters the artial blood pool with concentration

$$C_{a''} = C_{a'}(1 - Q_{fs}) + C_v Q_{fs}.$$

For the arterial blood pool, the change in concentration is

$$\frac{dC_a}{dt} = \frac{Q_{CO}(C_{a''} - C_a)}{V_{bla}},$$

which is then distributed to the major tissue compartments. The tissue compartments can be described similarly as

$$\frac{dC_t}{dt} = \frac{Q_t(C_a - C_t)}{V_t \lambda_t}$$

where the subscript t denotes one of the seven tissue types.

The venous blood draining the brain, heart, kidney, and liver (i.e. viscera) combines and enters a blood pool, called the *venous pool viscera*, with concentration

$$C_{vpv} = \frac{C_b Q_b + C_h Qh + C_k Q_k + C_l Q_l}{Q_b + Q_h + Q_k + Q_l}.$$

The blood exiting the *venous pool viscera* then has concentration

$$\frac{dC_{vpv}}{dt} = \frac{(C_{vpv} - C_{vpv'})(Q_b + Q_h + Q_k + Q_l)}{V_{vpv}}.$$

The next major tissue groups, muscle and connective tissue, drain into a blood pool called the *venous pool lean tissue*. The concentration entering this pool is

$$C_{vpl} = \frac{C_m Q_m + C_{ct} Q_{ct}}{Q_m + Q_{ct}}$$

and leaving

$$\frac{dC_{vpl'}}{dt} = \frac{(C_{vpl} - C_{vpl'})(Q_m + Qct)}{V_{vpl}}.$$

The last tissue group, adipose tissue, drains into the *venous pool adipose* with concentration C_{at}. The concentration leaving the pool is

$$\frac{dC_{at}}{dt} = \frac{(C_a - C_{at})Q_{at}}{V_{at}\lambda_{at}}.$$

Finally, the venous blood from the three venous pools is collected into the central venous pool. Their combined concentration is

$$C_{v'} = \frac{C_{vpv'}(Q_b + Q_h + Q_k + Q_l)}{Q_{CO}} \quad (1)$$

$$+ \frac{C_{vpl'}(Q_m + Q_{ct})}{Q_{CO}} + \frac{C_{vpa'} Q_{at}}{Q_{CO}}. \quad (2)$$

The concentration leaving the central venous pool and returning to the lungs is

$$\frac{dC_v}{dt} = \frac{(C_{v'} - C_v)Q_{CO}}{V_{vpc}},$$

concluding the family of equations that describe the model.

It has also been shown that $PaCO_2$influences cerebral blood flow, and so the following exponential relationship will be used to alter cerebral blood flow as a function of $PaCO_2$.

$$CBF = 4.29e^{0.0589 EtCO_2},$$

where CBF is cerebral blood flow in $\text{ml} \cdot \text{min}^{-1} \cdot 100\text{g}^{-1}$ and $PaCO_2$has been estimated using the easily measured $EtCO_2$ (mmHg)[17].

The model will be evaluated in Simulink (Mathworks, Natick, MA). Figure 1(c) shows the equivalent Simulink model for the basic model described in the Figures 1(a) and 1(b). Besides its intuitive graphical interface for constructing models, another useful feature in Simulink is its modular approach to building complex models. The basic model in Figure 1(c) can be encapsulated in its own block or module, and then a series of these modules can be interconnected to form the network that describes the model in Figure 2. The equivalent Simulink model is shown in Figure 3.

III. Results

The plot in Figure 4 shows a simulation of anesthetic concentrations during surgery, emergence, transport, and recovery of a typical patient. The blue line shows the concentration of inspired agent as recorded by the anesthesia machine. The red and cyan show the simulated arterial and cerebral concentrations. The purple and green lines show the measured and simulated end tidal anesthetic concentration respectively .

At the beginning of surgery, the clinician usually gives a high dose of agent concentration in order to quickly reach

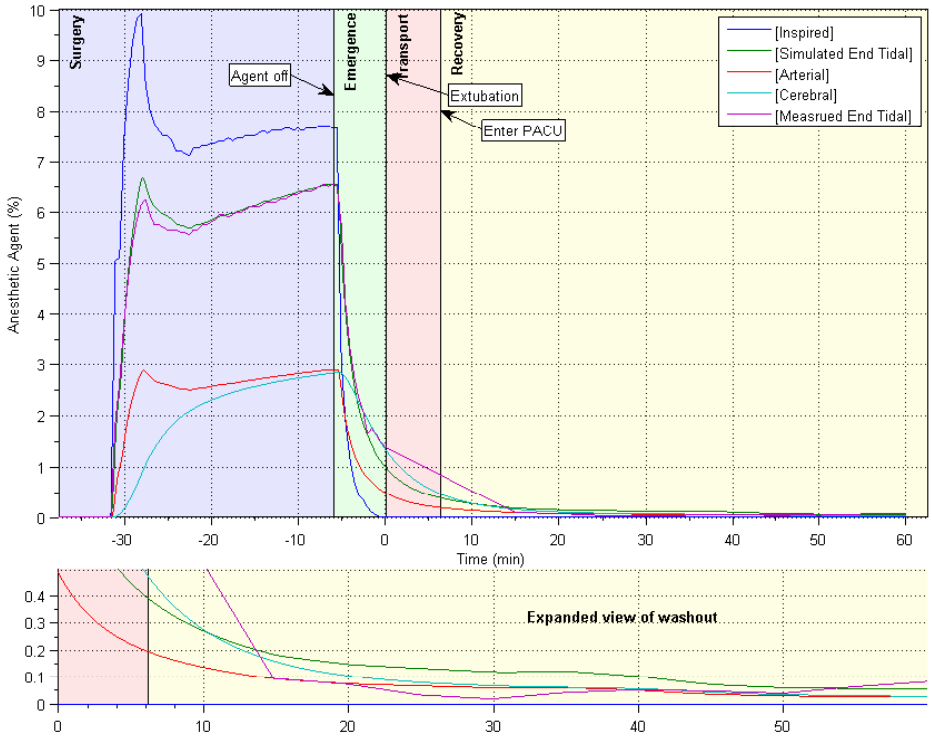

Fig. 4. Simulation of anesthetic concentration for a typical patient. Note the close approximation of the simulated end tidal anesthetic agent to the measured one (purple and green lines respectively). The blue line shows the inspired concentration. The red and cyan lines show the arterial concentration and cerebral concentration respectively. The cerebral concentration is modeled as a function of $PaCO_2$. The bottom graph shows an expanded view of the washout period during recovery.

the maintenance value of 6% end tidal agent concentration as quickly as possible. Often this results in a brief overshoot, as seen as the spike in concentration at the beginning of the case.

It can also be seen that the simulated end tidal concentration nearly approximates the measured end tidal concentration. This is most evident during the surgery and emergence periods. During the transport period, when the patient is being disconnected from the anesthesia equipment and moved to the PACU, the approximation differs more, but then seems to merge again during recovery.

The bottom smaller graph shows an expanded view of the recovery period. In this view it can be seen that the simulated curve is slightly higher than the measured curve for nearly the entire period.

When a paired *t*-test was performed on the end tidal data for the surgery and emergence periods for 18 patients enrolled in the study thus far, the difference between the simulated and measured data was not significant, but during the transport and recovery periods the difference was significant—despite the apparent small difference shown in the expanded view.

IV. Discussion

During the surgery and emergence periods, the patient data (i.e. $EtCO_2$, end tidal and inspired agent concentration, and MV) is recorded at a sample frequency of 30 sec. During transport period, no data is recorded because no monitors can be connected while the patient is moved from the OR to the PACU. Once the patient enters the PACU and is situated the sample frequency is 100 Hz. However, for this first set of simulations, data points taken every 5 min during recovery were used. This was because at every 5 min interval a calibration test was performed using a gas analyzer and spirometer to calibrate the second monitor—a device used to measure minute volume using only inductance through elastic bands placed around the chest and abdomen (this is so that patients were not required to wear an airtight mask during recovery). The data available via the gas analyzer and spirometer during the calibration periods was readily available for use in the simulation. The higher resolution data, after some work, can be made available for use in the simulation. And after performing the *t*-test, it is apparent that the higher resolution data should be used to see if it improves the model.

The two main driving forces behind washout are ventilation and cardiac output. As was mentioned, during transport no data is recorded; and as illustrated in Figure 4 by the measured end tidal signal, data points in the minute volume signal were linearly interpolated as an initial attempt to compensate for the lack of data. A better interpolation method could probably be devised, although it is not really known how minute volume changes during transport. Cardiac output could also be modified to improve the model.

In the original 1991 Lerou model, cardiac output was approximated as constant, estimated as a fraction of body weight, which was also used in this model for simplicity sake[1].

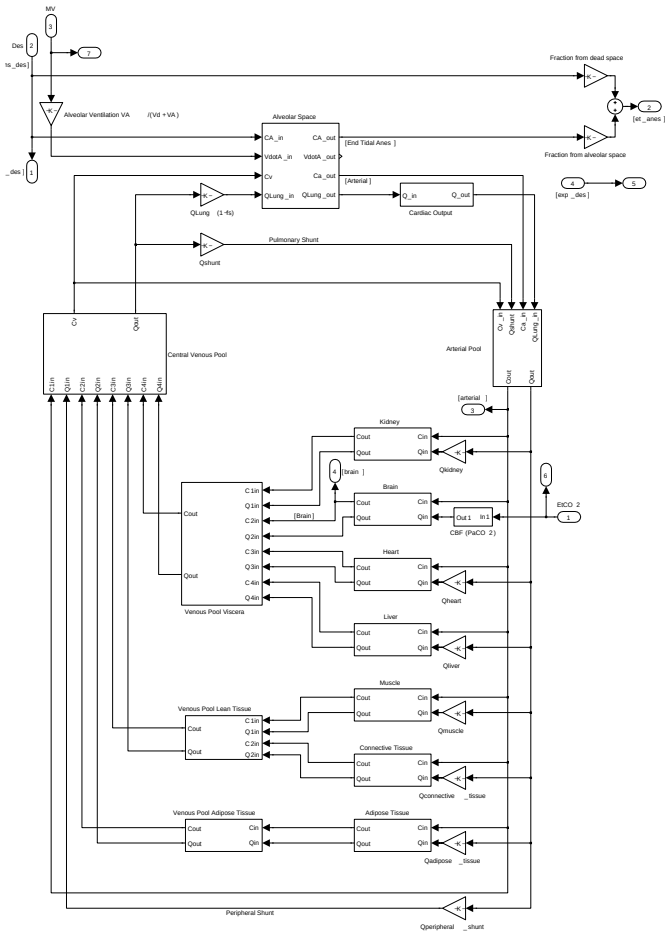

Fig. 3. Simulink model describing the uptake, distribution, and washout of inhaled anesthetic.

However, since then studies have shown how cardiac output can be influenced by $PaCO_2$. In Gopalakrishnan's dissertation, he derived a relationship between cardiac output and $PaCO_2$ based on measured data[14]. Implementing this relationship might also improve washout.

V. Conclusions

While the model overall appears to simulate anesthetic concentrations well, especially during the surgery and emergence periods, the discrepancies seen in the transport and recovery periods are different enough to be significant and need to be addressed before this model can be used to effectively explore anesthetic washout during recovery.

Acknowledgments

The author would like to thank Dr. Dwayne Westenskow, Dr. Joseph Orr, Dr. Derek Sakata, for their direction and involvment in this project, as well as those involved in the data collection at the Moran Eye Center.

References

[1] J. G. Lerou, R. Dirksen, H. H. Beneken Kolmer, and L. H. Booij, "A system model for closed-circuit inhalation anesthesia. i. computer study," *Anesthesiology*, vol. 75, no. 2, pp. 345–55, Aug 1991.

[2] E. I. Eger, 2nd and L. J. Saidman, "Illustrations of inhaled anesthetic uptake, including intertissue diffusion to and from fat," *Anesth Analg*, vol. 100, no. 4, pp. 1020–33, Apr 2005.

[3] D. J. Sakata, N. A. Gopalakrishnan, J. A. Orr, J. L. White, and D. R. Westenskow, "Hypercapnic hyperventilation shortens emergence time from isoflurane anesthesia." *Anesth Analg*, vol. 104, no. 3, pp. 587–591, 2007.

[4] ——, "Rapid recovery from sevoflurane and desflurane with hypercapnia and hyperventilation." *Anesth Analg*, vol. 105, no. 1, pp. 79–82, 2007.

[5] H. Ito, I. Kanno, M. Ibaraki, J. Hatazawa, and S. Miura, "Changes in human cerebral blood flow and cerebral blood volume during hypercapnia and hypocapnia measured by positron emission tomography." *J Cereb Blood Flow Metab*, vol. 23, no. 6, pp. 665–670, Jun 2003.

[6] K. Ide, M. Eliasziw, and M. J. Poulin, "Relationship between middle cerebral artery blood velocity and end-tidal pco2 in the hypocapnic-hypercapnic human ranges," *J Appl Physiol*, vol. 95, pp. 129–137, 2003.

[7] J. E. J. Brian, "Carbon dioxide and the cerebral circulation." *Anesthesiology*, vol. 88, no. 5, pp. 1365–1386, 1998.

[8] R. R. Blocker, D. J. Sakata, N. A. Gopalakrishnan, J. A. Orr, and D. R. Westenskow, "Clinical evaluation of the qed-100 emergence device," *Anesthesiology*, vol. 105, no. A853, 2006.

[9] D. J. Sakata, N. Gopalakrishnan, J. A. Orr, and J. White, "Clinical evaluation of a device to speed emergence from sevoflurane anesthesia," *Anesthesiology*, vol. 103, p. A796, 2005.

[10] D. Sakata, J. Orr, and D. Westenskow, "Clinical evaluation of a device to speed emergence from inhaled anesthetic," *Anesthesiology*, vol. 99, p. A576, 2003.

[11] R. Hines, P. G. Barash, G. Watrous, and T. O'Connor, "Complications occurring in the postanesthesia care unit: a survey." *Anesth Analg*, vol. 74, no. 4, pp. 503–509, 1992.

[12] D. K. Rose, M. M. Cohen, D. F. Wigglesworth, and D. P. DeBoer, "Critical respiratory events in the postanesthesia care unit. patient, surgical, and anesthetic factors." *Anesthesiology*, vol. 81, no. 2, pp. 410–418, 1994.

[13] S. E. Tarrac, "A description of intraoperative and postanesthesia complication rates," *J Perianesth Nurs*, vol. 21, no. 2, pp. 88–96, Apr 2006.

[14] N. Gopalakrishnan, "Hypercapnic hyperventilation speeds emergence from inhaled anesthesia," Ph.D. dissertation, University of Utah, 2006.

[15] J. G. Lerou, R. Dirksen, H. H. Beneken Kolmer, L. H. Booij, and G. F. Borm, "A system model for closed-circuit inhalation anesthesia. ii. clinical validation," *Anesthesiology*, vol. 75, no. 2, pp. 230–7, Aug 1991.

[16] T. H. Hallynck, H. H. Soep, J. A. Thomis, J. Boelaert, R. Daneels, and L. Dettli, "Should clearance be normalised to body surface or to lean body mass?" *Br J Clin Pharmacol*, vol. 11, no. 5, pp. 523–6, May 1981.

[17] F. Mielck, H. Stephan, W. Buhre, A. Weyland, and H. Sonntag, "Effects of 1 mac desflurane on cerebral metabolism, blood flow and carbon dioxide reactivity in humans." *Br J Anaesth*, vol. 81, no. 2, pp. 155–160, Aug 1998.